



## Article

# Software Program for the Evaluation of Human Exposure to Electric and Magnetic Fields

Adina Giurgiuman <sup>1,2,\*</sup>, Marian Gliga <sup>1,2</sup>, Adrian Bojita <sup>1,2</sup>, Sergiu Andreica <sup>1</sup>, Calin Munteanu <sup>1</sup>, Vasile Topa <sup>1</sup>, Claudia Constantinescu <sup>1</sup> and Claudia Pacurar <sup>1</sup>

- <sup>1</sup> Department of Electrotechnics and Measurements, Faculty of Electrical Engineering, Technical University of Cluj-Napoca, 400114 Cluj-Napoca, Romania; marian.gliga@ethm.utcluj.ro (M.G.); adrian.bojita@ethm.utcluj.ro (A.B.); sergiu.andreica@ethm.utcluj.ro (S.A.); calin.munteanu@ethm.utcluj.ro (C.M.); vasile.topa@ethm.utcluj.ro (V.T.); claudia.constantinescu@ethm.utcluj.ro (C.C.); claudia.pacurar@ethm.utcluj.ro (C.P.)
- <sup>2</sup> Academy of Romanian Scientists, Ilfov 3, 050044 Bucharest, Romania
- \* Correspondence: adina.giurgiuman@ethm.utcluj.ro

**Abstract:** The evaluation of human exposure to electric and magnetic fields represents a subject of great scientific and public interest due to the biological effects of electromagnetic fields (EMFs) on the human body and the risks caused by them to living organisms. In this context, this article proposes a software program designed by the authors for the evaluation of human exposure to electric and magnetic fields at low frequencies (EMF software program), an application that can also be accessed from a mobile phone. The analytical model on which the EMF program is based is synthetically presented, and the application is then described. The first example implemented in the EMF program is taken from the existing literature on this subject, thus confirming the correctness and calculation precision of the program. Next, a case study is proposed for an overhead transmission line of 400 KV from the Cluj-Napoca area, Romania, for which the electric and magnetic fields are first measured experimentally and then using the EMF program. The validation of the EMF software program is performed by comparing the obtained results with those measured experimentally and with those obtained with a commercial software program.



**Citation:** Giurgiuman, A.; Gliga, M.; Bojita, A.; Andreica, S.; Munteanu, C.; Topa, V.; Constantinescu, C.; Pacurar, C. Software Program for the Evaluation of Human Exposure to Electric and Magnetic Fields.

*Technologies* **2023**, *11*, 159.

<https://doi.org/10.3390/technologies11060159>

Academic Editor: Valeri Mladenov

Received: 2 October 2023

Revised: 24 October 2023

Accepted: 25 October 2023

Published: 8 November 2023

**Keywords:** human exposure; electric field; magnetic field; electromagnetic compatibility; calculation algorithms; overhead transmission line

## 1. Introduction

The exponential technological development of the last few years has led to the overall development of society and, at the same time, to an increase in the comfort and quality of daily life for each of us. It should be emphasized that this development is directly based on increasing electricity consumption in parallel with the search for new, clean, green energy sources. When we talk about pollution, we usually think only about the pollution caused by carbon emissions and greenhouse gases and neglect an also important and increasing pollution source, namely electromagnetic pollution. This results from increased electricity consumption and is manifested by the existence of an electromagnetic field (EMF) in the vicinity of any equipment that uses electrical energy. It has been proven that the electromagnetic fields in the vicinity of electro-energetic equipment affect people, causing different effects. As such, exposure to electromagnetic fields is regulated by a Directive of the European Union; thus, it must be measured and monitored, both in areas considered for the general exposure of the population (areas located near transmission and distribution power lines), where, in Romania, the provisions given by the Order of the Ministry of Public Health, WHOP 1193 of 29 September 2006, on limiting the exposure of the population to electromagnetic fields from 0 Hz to 300 GHz must be observed [1], and in areas in which there is considered to be a professional exposure (the premises of electrical transformer



**Copyright:** © 2023 by the authors. Licensee MDPI, Basel, Switzerland. This article is an open access article distributed under the terms and conditions of the Creative Commons Attribution (CC BY) license (<https://creativecommons.org/licenses/by/4.0/>).

stations); this is where, in Romania, the provisions contained in Government Decision GD 520/2016 on the minimum safety and health requirements regarding the exposure of workers to the risks posed by electromagnetic fields [2] must be observed.

The evaluation of human exposure to electric and magnetic fields is a subject of great interest worldwide, as can be seen from the attached bibliographic list. The biological effects of electromagnetic fields on the human body were and still are a subject of both scientific and public interest, considering their risks to living organisms; these risks are presented in [3–9].

The calculation of the electromagnetic field around and in the proximity of overhead transmission lines, which pass over some houses, factories, and schools, is presented in [10], while in [11], the authors present field monitoring in the area and in the immediate vicinity of a high-voltage (HV) substation in Novi Sad, Serbia.

The effect of human exposure to the magnetic field generated by an electricity transport and distribution overhead transmission line is also studied in [12], and in [13], Ghervenkov presents an evaluation of the electric and magnetic fields generated by an overhead transmission line (OHTL) in an urban area of Bulgaria.

S.M. Ghania, in [14], presents an analytic and numeric evaluation of the potential risk posed by electromagnetic fields emitted in the interior of an HV station, this being considered a subject of great interest for designers and biomedical researchers in the field. In [15], analytical and numerical methods for the calculation of the electric and magnetic field distribution in the proximity of electrical installations' equipment from HV stations are presented.

Of great importance in the evaluation of human exposure to electric and magnetic fields are also the standards in force. In this context, in [16,17], the most-used standards in this field are presented together with different methods to calculate the parameters involved in these evaluations.

Experimental and numerical evaluations of electric and magnetic fields are presented in [18], in the area of an electric station in Xanthi, Greece; in [19], in a station in Jingmen, China; in [20], in a station in Finland; in [21–23], in different stations in Romania; in [24], in a station in the north-east of Brazil; in [25], in a station in Libya; and in [26], in the area of an OHTL in Bosnia and Herzegovina.

All this research in the domain of human exposure to electric and magnetic fields through analytic, numeric, and/or experimental methods presented in the articles mentioned above confirm the actuality of the subject addressed in this article.

In this light, the main aim of this article is the development, implementation, and testing of a software application dedicated to the evaluation of human exposure to electric and magnetic fields that is also able to be accessed on a mobile phone.

The concept for this study derives from the growing demands of the private companies that contribute to the retrofitting of electrical substations for the assessment of human exposure to electric and magnetic fields in these stations. In addition, we cannot neglect the requests that we have had over the years for the assessment of electric and magnetic fields in urban areas crossed by OHTLs. In the process of evaluating the exposure of humans to electric and magnetic fields, we have measured the high values of electric and magnetic fields many times and asked ourselves whether the measured value is the real one or whether it is a measurement error, or whether there are other electromagnetic fields emitted by devices/sources near the test area. These measured values can be influenced by the presence of underground cables, by meteorological factors, and also by other devices functioning at the industrial frequency, 50 Hz.

In order to provide a rapid answer to this question, in the field, in precisely the place the electromagnetic compatibility (EMC) tests were carried out, we considered that it would be useful to design and develop a software application to determine electric and magnetic fields at low frequencies, and that this application should be easily accessed even from a mobile phone; this is how the EMF application was born.

Section 1 highlights the novelty and importance of the subject addressed in this paper. In Section 2, the calculation algorithms for the electric and magnetic field are presented, along with the analytical models and the design and implementation of the EMF software program. Section 3 consists of a case study on an OHTL of 400 kV in Cluj-Napoca, Romania, where the electric and magnetic field were determined using three different methods: experimentally, using the EMF software program developed by the authors, and using a commercial software program. In Section 4, the EMF software program is tested and validated by comparing the results obtained using the three methods and by calculating the error percentages. The final conclusions of this study are presented in Section 5.

## 2. Materials and Methods

### 2.1. Calculation Module of the Electric and Magnetic Field Generated by a Transmission and Distribution Electric Line

The EMF software program was designed so that it could determine the electric potential, the electric field intensity, and the magnetic induction values from the proximity of the transmission and distribution electric lines. For the development, conception, and implementation of this application, it was necessary, first of all, to develop an analytic module for calculating the electromagnetic field.

The electromagnetic field in the proximity of conductors and bars from a high or very high voltage varies in time with a low frequency, with a value of 50 Hz in Europe (called industrial frequency); thus, the wavelength of the field is 6000 km. The practical consequence of this wavelength is the fact that the electromagnetic field radiant properties can be neglected. From this point of view, the difference between the electromagnetic field at a low frequency and the electromagnetic field at a high frequency is that microwaves, radars, or radio waves can be clearly observed. The wavelength, being significantly larger than the characteristic dimensions of the exposed organisms, and the skin depth of the field in biological environments, being greater than these dimensions, enable the application of the theory of the quasi-stationary electromagnetic field in linear environments. The approximation of the solutions to Maxwell's equations can be made with an extremely small error ( $2 \times 10^{-6}\%$ ), in comparison to the real situation, if this theory is applied to determine the fields at distances up to 100 m from an OHTL [27–29].

Thus, as is clear from the ideas presented above and from a study of the literature in the field of interest [12,13,15,18,19,21–24,26], it is well known that in the assessment of the electromagnetic field generated by an OHTL, the stationary operating regime of the electromagnetic field is considered valid, so the electric field and magnetic field are analyzed and treated independently.

In this context, the following paragraphs will present the analytical expressions and the implemented algorithms used to analytically and numerically determine the electric and magnetic fields generated in the proximity of the OHTL.

#### 2.1.1. Calculation Module of the Electric Field Generated by OHTL

The calculation of the electric field in the proximity of the OHTL (and station bars) was performed by starting with the theory of long and thin conductors in the presence of the ground [27,28].

Starting with the fundamental laws of the electromagnetic field, the expression for the electric potential distribution of a filiform conductor can be determined for the case in which the conductor's potential is set as  $V_0$  [29]:

$$V = V_0 \frac{\ln \frac{r_2}{r_1}}{\ln \frac{2h}{r_0}} \quad (1)$$

where:

- $r_1$  is the distance from the real conductor to the calculation point;
- $r_2$  is the distance from the image conductor to the calculation point;

- $h$  is the distance from the ground to the real conductor;
- $r_0$  is the conductor radius.

Finally, the expression of the potential distribution for the case of a three-phase power line is as follows:

$$\underline{V} = V_0 \sum_{k=1}^3 e^{j\frac{2k\pi}{3}} \frac{\ln \frac{r_{2k}}{r_{1k}}}{\ln \frac{2h_k}{r_{0k}}} \quad (2)$$

where:

- $r_{1k}$  is the distance from each real conductor to the calculation point;
- $r_{2k}$  is the distance from each image conductor to the calculation point;
- $h_k$  is the distance from the ground to each real conductor;
- $r_{0k}$  is the radius of each conductor.

To exemplify the configuration of the three-phase OHTL considered in the relationships involved in the analytical models for the calculation of the electric potential and the respective electric field intensity, Figure 1 shows a sketch of the considered model.

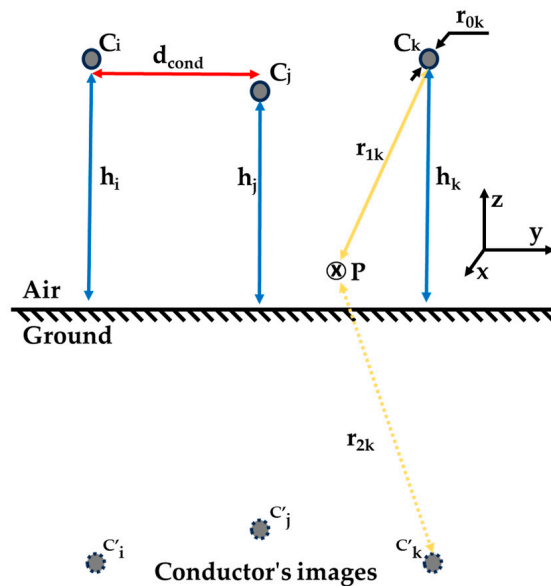


Figure 1. The geometrical configuration of the studied problem.

To determine the calculation expression of the electric field intensity, if we consider the case of a single conductor, the calculation relationship is as follows [27]:

$$\bar{E} = \frac{V_0}{\ln \frac{2h}{r_0}} \left( \frac{\bar{r}_2}{r_2^2} - \frac{\bar{r}_1}{r_1^2} \right) \quad (3)$$

and in the case of a three-phase power line, the expression is determined by overlapping the effects as follows [29]:

$$\bar{E} = V_0 \sum_{k=1}^3 e^{j\frac{2k\pi}{3}} \frac{\left( \frac{\bar{r}_{2k}}{r_{2k}^2} - \frac{\bar{r}_{1k}}{r_{1k}^2} \right)}{\ln \frac{2h_k}{r_{0k}}} \quad (4)$$

### 2.1.2. Calculation Module of the Magnetic Field Generated by OHTL

To determine the calculation expression for the magnetic field intensity in proximity to the OHTL, the theory of long and thin conductors was also used. Therefore, in order

to determine the magnetic field intensity in the case of a filiform conductor, the following well-known relation can be used [27,28]:

$$\bar{H} = \frac{I}{2\pi r^2} \bar{r}_1 \quad (5)$$

where:

- $r$  is the distance from the conductor to the calculation point;
- $\bar{r}_1$  is a vector of the module equal to  $r$ , but rotated from the position vector  $\bar{r}$  with  $\pi/2$  in a trigonometric reverse direction.

In these conditions, in the case of the three-phased OHTL, the calculation relation becomes the following [27,29]:

$$\bar{H} = \frac{I}{2\pi} \sum_{k=1}^3 e^{j\frac{2k\pi}{3}} \frac{\bar{r}_{1k}}{r_k^2} \quad (6)$$

Based on these relations, we can finally determine the calculation expression of the magnetic induction for the three-phased OHTL:

$$\bar{B} = \mu_0 \frac{I}{2\pi} \sum_{k=1}^3 e^{j\frac{2k\pi}{3}} \frac{\bar{r}_{1k}}{r_k^2} \quad (7)$$

## 2.2. The EMF Software Program

The software application for the human exposure to electric and magnetic fields assessment, named EMF, allows us to determine the electric potential (V), the electric field intensity (E), the magnetic field intensity (H), and also the magnetic induction (B), both in points and along the calculation/measurement path. Also, with the help of the EMF program, we can obtain the electric and magnetic field distribution on a surface between two poles, making it possible to represent the calculated values in 1D or 2D.

The determination of the electric and magnetic field is carried out in numerical form, adapted for different LEA configurations; this is so that its geometric parameters (distances, heights, sections, coordinates for the calculation points, etc.) and electric parameters (electrical voltage, electric current intensity) can be easily modified by users. The calculation algorithm (back-end) is made with the programming language PYTHON 3.11 and is based on the analytical calculation expressions presented in the paragraphs above. PYTHON 3.11 programming language was chosen because many libraries with mathematical functions for scalar and vectorial calculations, as well as many useful libraries for creating graphic and post-process representations of the results, are available to its users.

The graphical interface of the developed program uses the same programming language. The data are taken from the alphanumeric boxes in which the details of the studied model are introduced. The introduced data are stored in variables corresponding to each parameter. From the graphical interface of the developed program, presented in Figure 2, a section in the left of the window can be distinguished; this section is intended for entering data related to the analyzed project:

- Distance between the OHTL conductors;
- The height of the conductors from the ground;
- The height at which the calculations are made;
- The conductor's radius;
- The distance from the outside of the conductors up to that at which the analyses are made;
- The supply voltage of the conductors;
- The intensity of the electric current passing through the three conductors.

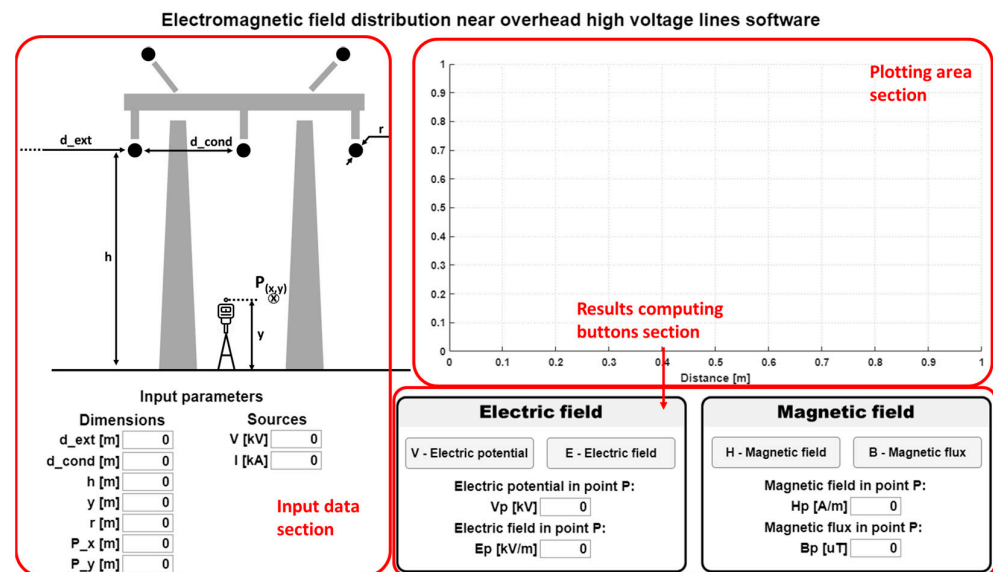


**Figure 2.** The interface of the EMF software program.

On the right side of the window, one can distinguish the display section for the variation plots of the electrical parameters, as well as the section of action buttons and the display of the calculated values at a point. A calculation can be reperfomed when pressing any button, so that closing the program window is not necessary.

This software program can also be accessed on a mobile phone, which greatly helps because it can also be used in the field, during EMC experimental measurements and tests. Practically, the EMF program includes two calculation modules: one for determining the electric field, which allows the assessment of the electric potential and the electric field intensity generated by the OHTL conductors, and the other one for determining the magnetic field, more precisely, the magnetic field intensity and magnetic induction.

### 2.2.1. The Calculation Algorithm for the Electric Field Generated by the OHTL

Following this, a study case analysis was conducted to assess the efficacy of the mathematical model integrated into the EMF program. The results obtained from the EMF program were compared with the previously validated measurements and numerical computations available in the literature [30], where a similar mathematical model was applied. This comparison established the utility and accuracy of the mathematical model integrated into the EMF program, as corroborated by the state-of-the-art research in the field. The study case presented in [30] considers the initial input data as follows:

- The height of the conductors from the ground (to the lines' sag),  $h = 11.2$  m;
- The distance between conductors,  $d_{\text{cond}} = 10.2$  m;
- The height of the calculation point P,  $y = 1.8$  m;
- The nominal voltage on the phase  $V_0 = 419$  kV;
- The nominal current on the phase is  $I_n = 151$  A.

The electromagnetic field calculation is performed for the entire width of the OHTL corridor, at a distance of 40 m, on both sides of the longitudinal axis of the corridor. These data were introduced into the EMF program and, in Figure 3, the electric field distribution is obtained for this case.

In Figure 4, the electric field distribution obtained using the EMF calculation program and the electric field distribution obtained in [30] are overlapped. By comparing the two sets of values, it can be observed that the calculation algorithm for the electric field implemented in the EMF program provides values approximately equal to those validated in the literature [30]. The difference between the values of the electric field E around the

$y = 0$  coordinate may come from the error in the conductor height measurements in [30], with the height being measured using an ultrasound device.

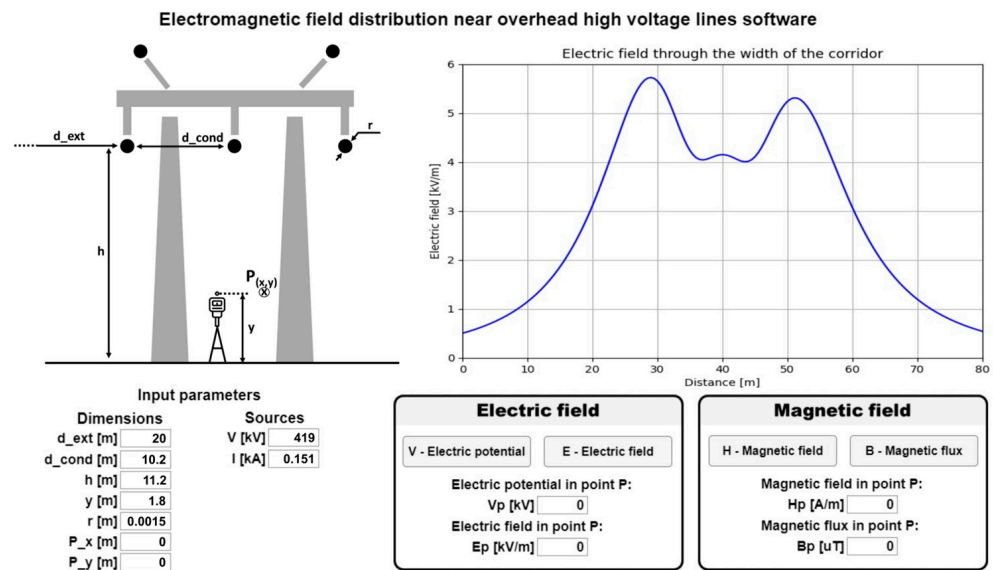


**Figure 3.** Electric field distribution obtained for the project taken from [30],  $f = 50$  Hz.

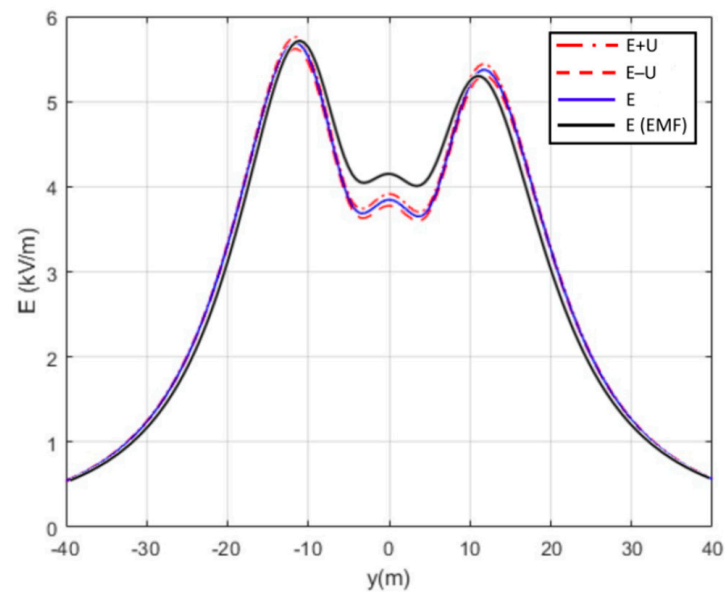


**Figure 4.** Comparison between the electric field distribution  $E$  on the width of the OHTL corridor taken from [30] and the electric field distribution  $E$  calculated using the EMF program,  $f = 50$  Hz.

### 2.2.2. The Calculation Algorithm of the Magnetic Field Generated by the OHTL

The same validation method was maintained to assess the computed magnetic field, like the one presented in Section 2.2.1. Therefore, the magnetic field generated by the OHTL measured in [30] was compared to that computed using the EMF program. The input data of the test case were the same.

The variation in the magnetic field obtained using the EMF program is presented in Figure 5, and in Figure 6, these results overlap with the ones taken from the literature [30], with the aim being to verify and validate the calculation algorithm for the magnetic field using the EMF program.

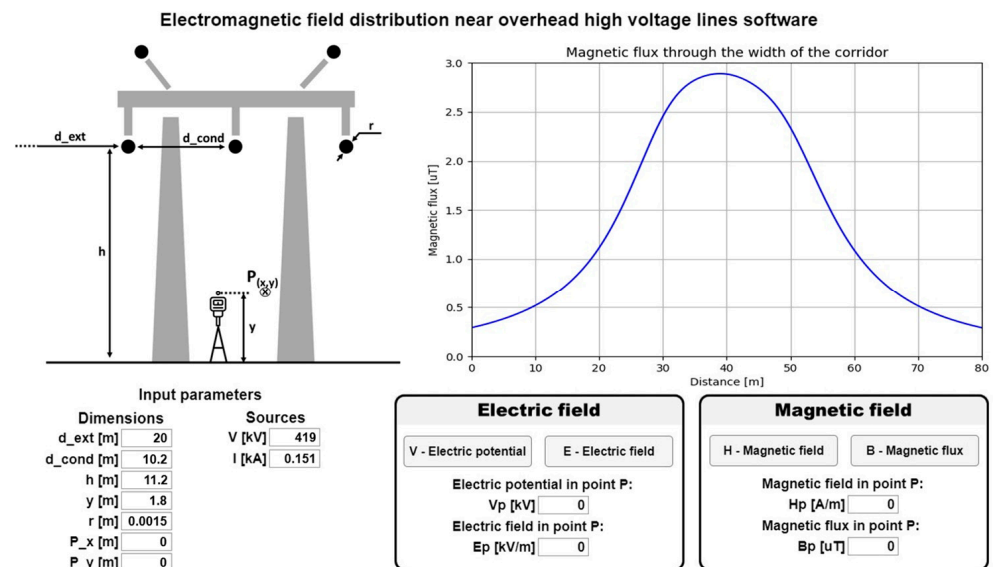


**Figure 5.** Magnetic field distribution obtained for the project taken from [30],  $f = 50$  Hz.

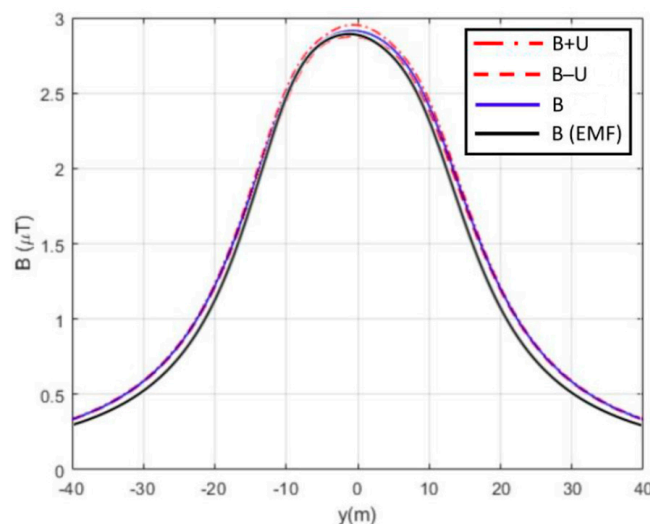


**Figure 6.** Comparison between the magnetic induction  $B$  on the width of the OHTL corridor taken from [30] and the magnetic induction calculated with the developed EMF program,  $f = 50$  Hz.

Comparing the two sets of values, it can be observed that the values of the magnetic induction  $B$  obtained using the EMF program are approximately equal to the ones obtained in [30] on the entire width of the OHTL corridor. Thus, we can say that our calculation algorithm for the magnetic field using the EMF program is more precise from the perspective of the calculated values.

### 3. Results

#### 3.1. Case Study—400 kV OHTL, Cluj-Napoca, Romania

In order to show the practical utility of the developed software program, and finally to verify and validate the results obtained using the EMF program, a 400 kV OHTL with a horizontal conductor configuration and in the vicinity of the city of Cluj-Napoca, Romania, was chosen as a case study. An area outside the town and far from any houses was chosen; this is because the purpose of carrying out these EMC tests was only to validate the software program developed and presented in this article. In order to obtain real geometrical data, a topographical analysis was carried out in the respective area, aiming in principle to determine the heights of the OHTL conductors for the three paths of interest considered,

perpendicular to the conductors; these were the 1st path (considered in the immediate vicinity of the pole, where the conductors, in this case, were located 27 m above the ground), the 2nd path (where a quarter of the lines sag, in which case the conductors are 14 m above the ground), and the 3rd path (the area of the maximum line sag, where the conductors are 11 m above the ground), as shown in the sketch in Figure 7.



**Figure 7.** Case study—explanatory calculation/measurement paths: (a) front view; (b) side view.

In Figure 8a, the measuring device for the measurement of the electric and magnetic field at a low frequency is presented; this was the Maschek ESM—100, which was made in Germany and used for the experimental measurements and EMC tests conducted on the three paths considered. The device is designed to measure the electric and magnetic fields associated with both transmission and distribution electrical installations and electrical devices for household and industrial use. Its frequency domain is between 5 Hz and 400 kHz, and regarding the measurement range, the device enables the measurement of the electric field intensity between 100 mV/m and 100 kV/m and the measurement of the magnetic induction between 1 nT and 20 mT. The measurements were made along the three paths of interest considered, from meter to meter, with each route considering 43 measuring points for a total of 129 measuring points.

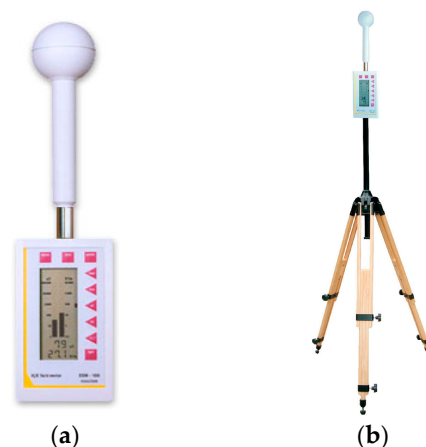


**Figure 8.** (a) Electric- and magnetic-field-measuring device, Maschek ESM—100; (b) explanation of experimental measurements.

Since the values of the electric field are influenced by the presence of people, the measuring device was placed on a tripod at the height of 1.8 m from the ground (Figure 8b), according to the requirements stipulated in the legislation and standards in force [1,2].

In order to obtain an overview of the distribution of the electric field and the measured magnetic field at the level of the area of interest considered, the measured values were imported into the TECPLOT program, a program that enables their three-dimensional representation. Thus, Figure 9a shows the overall distribution of the electric field in the

area between the pole and the lines' sag (that is, half of the distance between the two poles), and Figure 9b shows the distribution of the magnetic field in the same area.

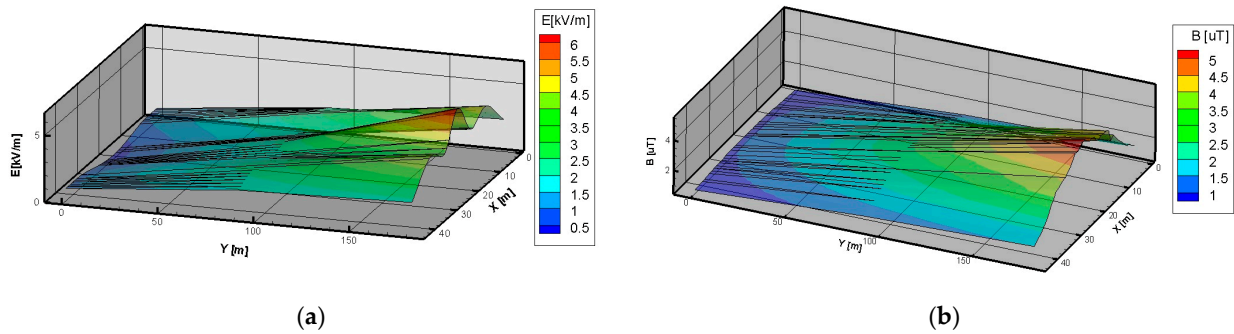


**Figure 9.** Experimental results: (a) electric field distribution in the tested area; (b) magnetic field distribution in the tested area,  $f = 50$  Hz.

Following the results presented in these images, we can observe that, as was expected, both the electric and magnetic field have low values on the first path when the conductors are at a high height from the ground, and that they reach a maximum value on the 3rd path, in the arow area.

For the analyses of the electric field distribution along each measurement path, Figure 10a–c show the distribution of the electric field along each path.

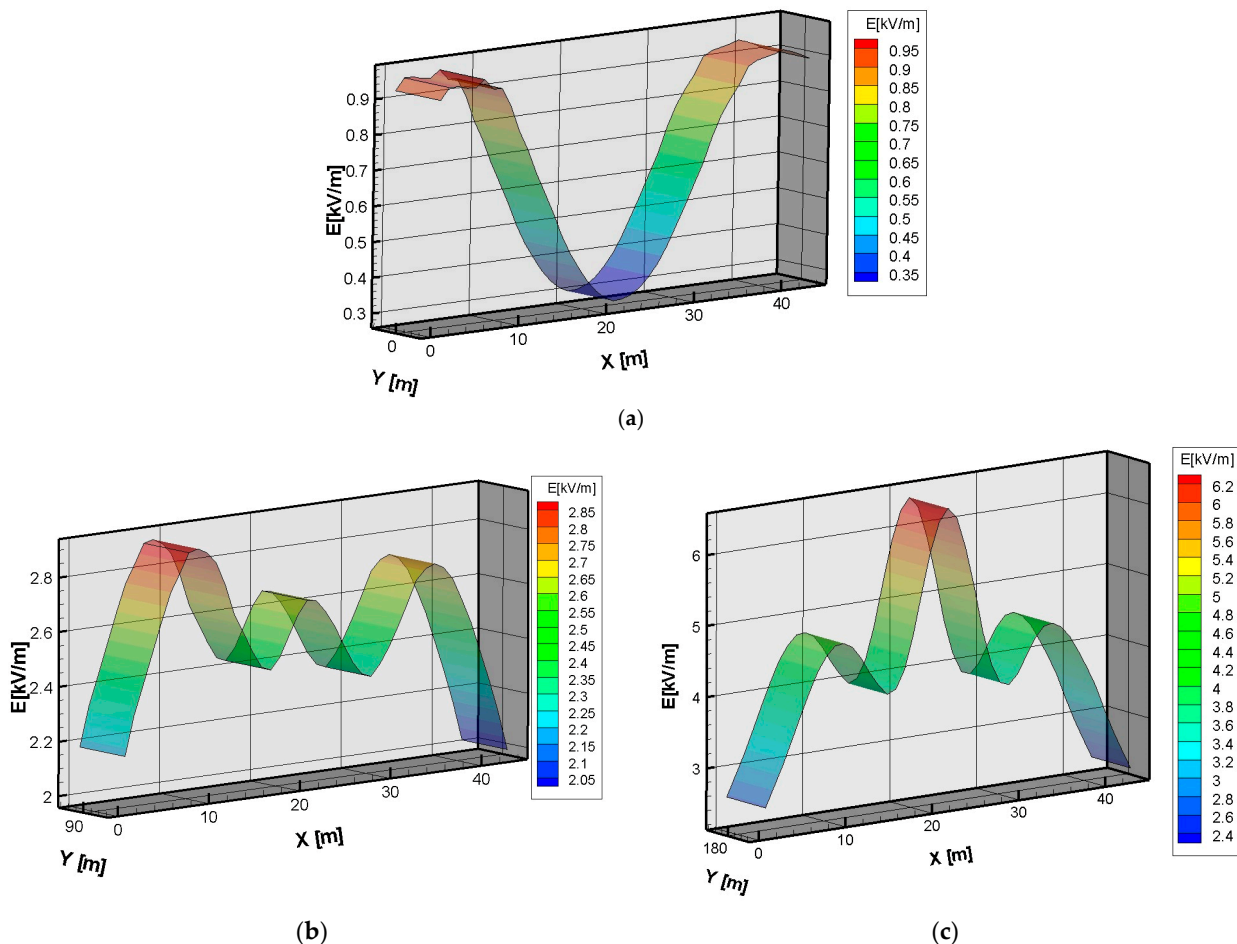


**Figure 10.** The electric field intensity distribution along the three paths experimentally determined: (a) 1st path,  $h = 27$  m; (b) 2nd path,  $h = 14$  m; (c) 3rd path,  $h = 11$  m,  $f = 50$  Hz.

It is interesting to note that, in the case in which the conductors are at a higher distance (27 m) from the testing height (1.7 m), meaning in the case of the 1st path, the values of the electric field are higher in the area from outside the conductors; meanwhile, for smaller heights, such as in the case of the 2nd path (14 m) and 3rd path (11 m), the distribution of the electric field is completely different. Also, taking into account the fact that the EMC testing area is outside the town, far from any houses, we can say that the results obtained comply with the legislation in force [1,2].

Similarly, in Figure 11a–c, the magnetic field distribution is presented along the three paths.

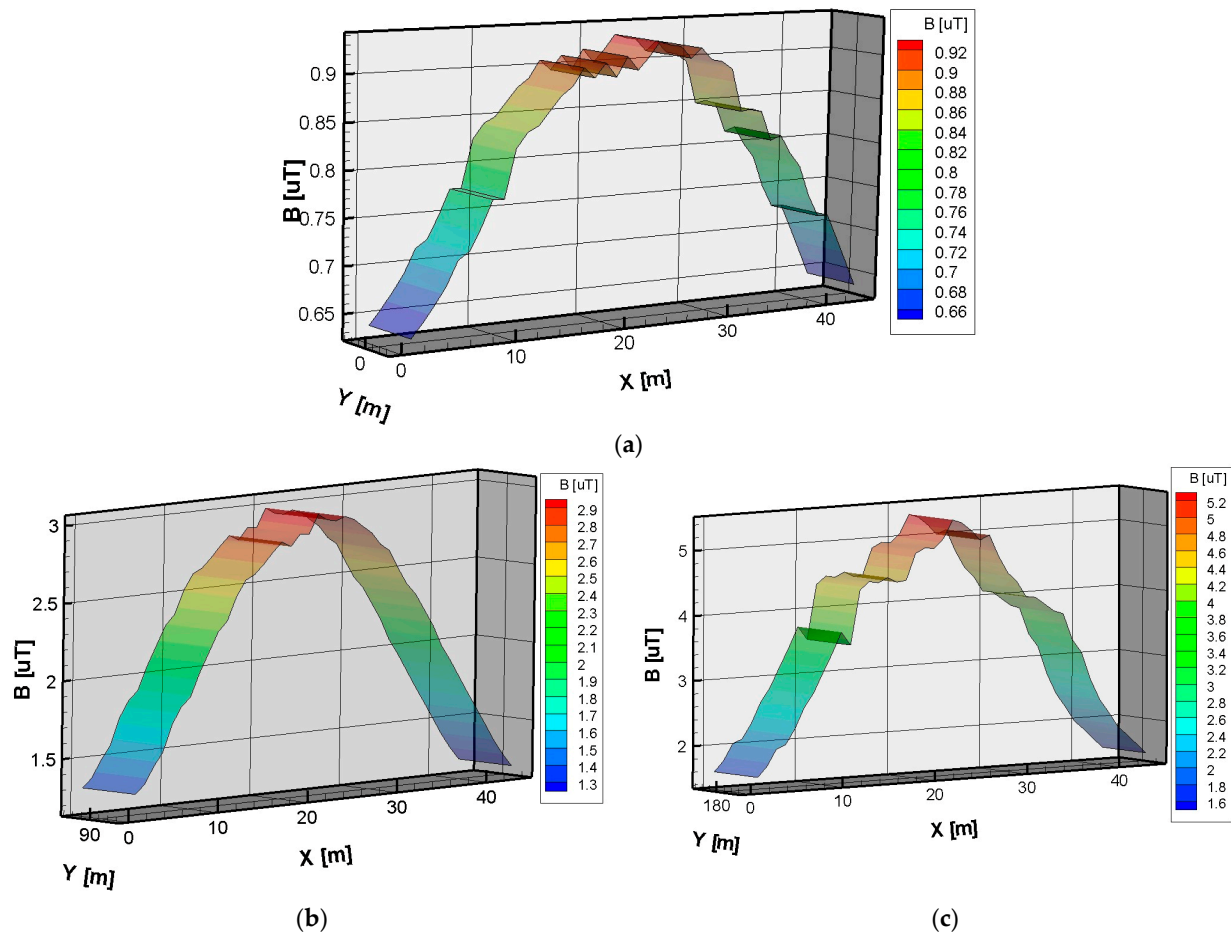


**Figure 11.** The magnetic induction distribution along the three paths experimentally determined: (a) 1st path,  $h = 27$  m; (b) 2nd path,  $h = 14$  m; (c) 3rd path,  $h = 11$  m,  $f = 50$  Hz.

By analyzing the results obtained, we can observe that, as expected, the higher values of the magnetic induction were obtained on the 3rd path, meaning that, for the case in which the OHTL conductors are 11 m from the ground, these values are within the limits imposed by the standards in force [1,2].

### 3.2. Determination of the Electric Field and the Magnetic Field Using the EMF Program

As mentioned above, the EMC tests for the presented case study were performed only to be able to validate and verify the results obtained using the EMF program developed by the authors. Therefore, the 400 kV OHTL experimentally analyzed in the paragraph above was implemented in the EMF program. Since the program also allows the calculation of the electric potential, Figure 12 shows its distribution on the three paths of interest considered. In the lower-left part of each image, we can identify some characteristic elements of the

400 kV OHTL model analyzed in Cluj-Napoca, which practically constitute the input data of the project.

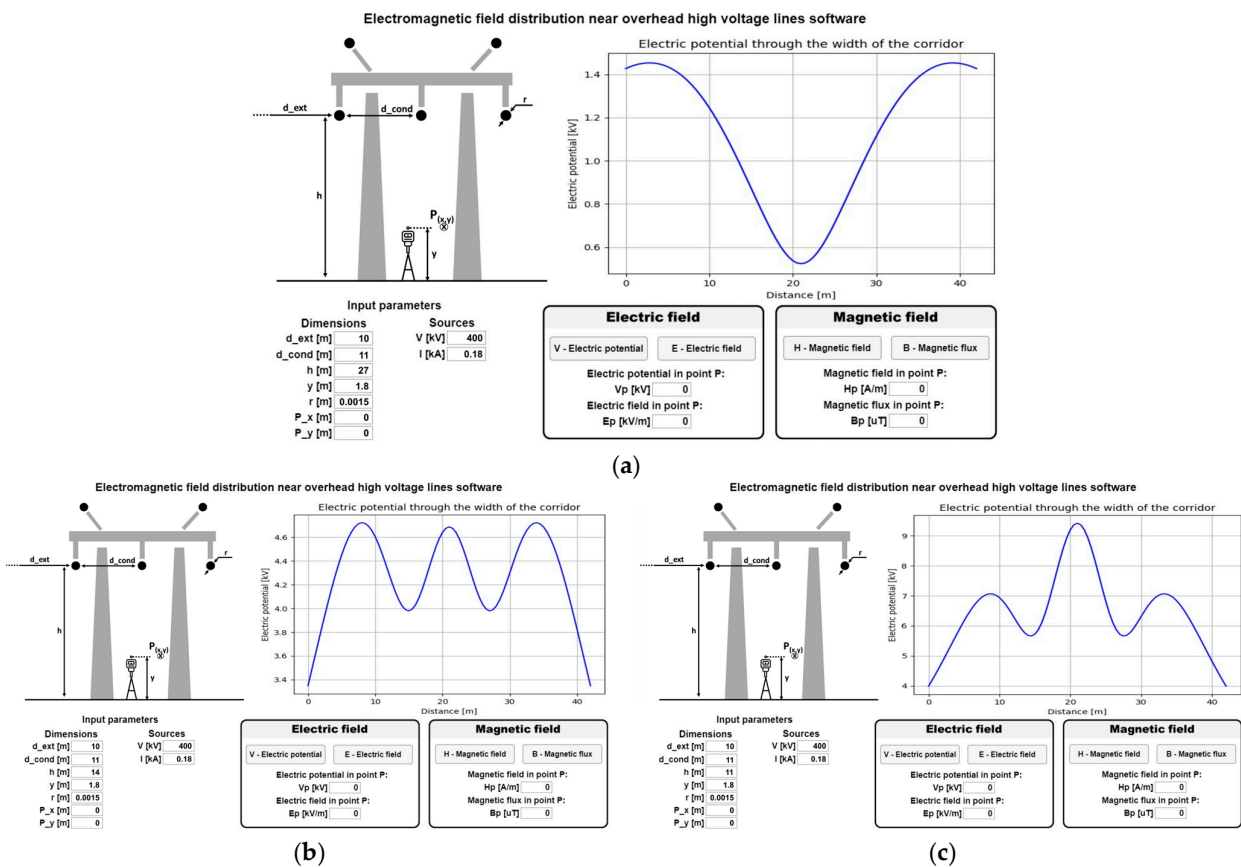


**Figure 12.** The electric potential distribution along the three paths, determined using the EMF program: (a) 1st path,  $h = 27$  m; (b) 2nd path,  $h = 14$  m; (c) 3rd path,  $h = 11$  m,  $f = 50$  Hz.

In Figure 13, the electric field distribution,  $E$ , is presented along the three paths of interest considered, highlighting the fact that, using the EMF software program, we can request that these calculations be made with a step smaller than 1 m, without the efforts that would be required to perform experimental measurements at more points. For example, in order to represent the electric field distributions presented below, calculations were made for 84 points on each path; in total, there were 254 calculation points, in contrast to the experimental tests in which we accumulated a total of 129 measurement points (43 points on each path).

Comparing the results obtained using the EMF software program (Figure 13) with those experimentally measured (Figure 10), we can observe that these are very similar.

In a similar way, in Figure 14, the magnetic field or magnetic induction obtained using the EMF software program developed by the authors along the three paths considered is presented.

The EMF software program enables values of interest, as well as some points, to be found, which is extremely important when we perform EMC tests and we want to know whether the measured value at an interest point is correct or whether there is a measurement error. To further highlight this facility offered by the EMF program, the values of the electric field in the three points of interest considered are presented in Figure 15; more precisely, the points placed under each of the three conductors of the OHTL at the height of 1.8 m from the ground are presented. In addition, in Figure 16, the values of the magnetic field obtained in the same points are presented.

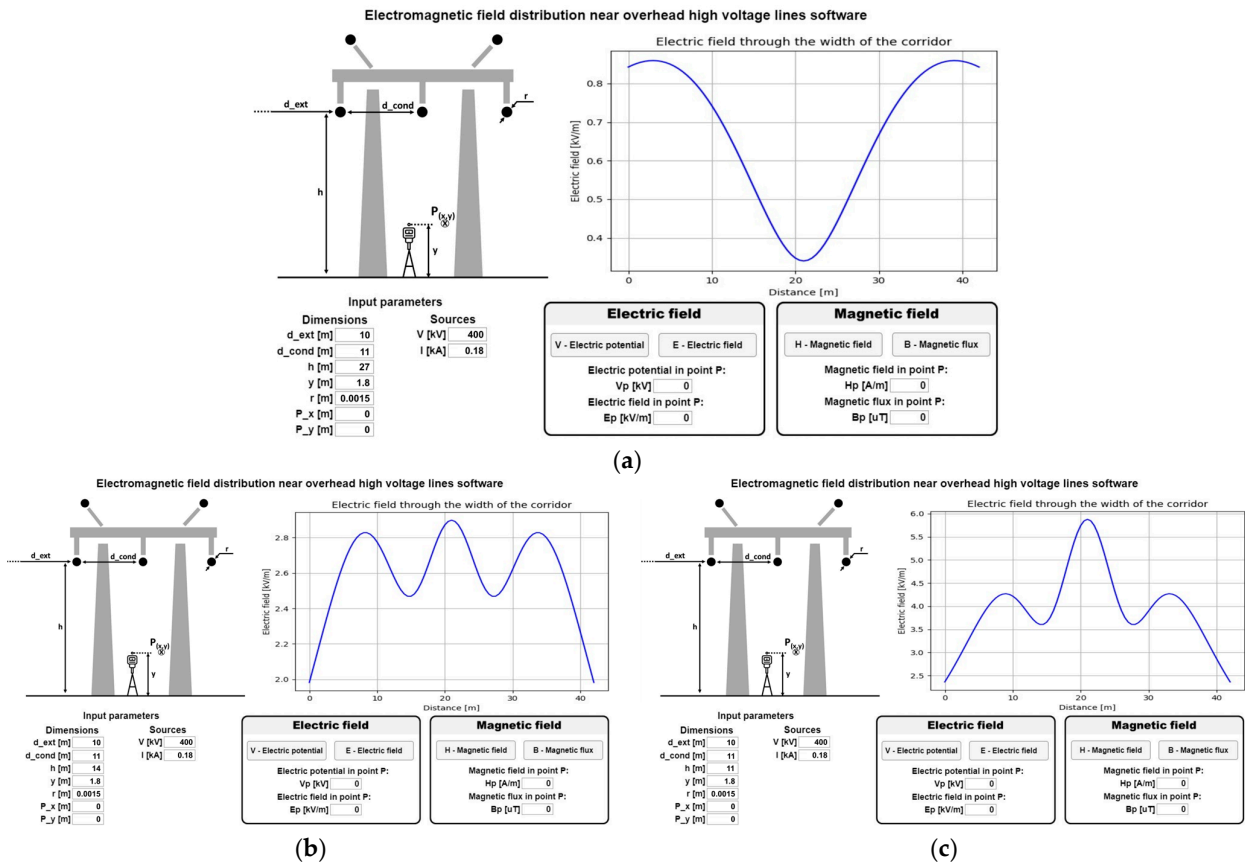


**Figure 13.** The electric field intensity distribution along the three paths, determined using the EMF program: (a) 1st path,  $h = 27$  m; (b) 2nd path,  $h = 14$  m; (c) 3rd path,  $h = 11$  m,  $f = 50$  Hz.

Using the EMF program, the electric and magnetic fields' distributions on an area between two pillars (poles) can also be determined. To further demonstrate these capabilities offered by the EMF program, the electric field distribution on the area between the two pillars for the 400 KV OHTL in Cluj-Napoca is presented. In Figure 17b, the magnetic field distribution in the same area is presented. To perform these distributions, the EMF program used a number of  $1.3 \times 10^5$  calculation points, for the determination of both the electric and magnetic field distributions.

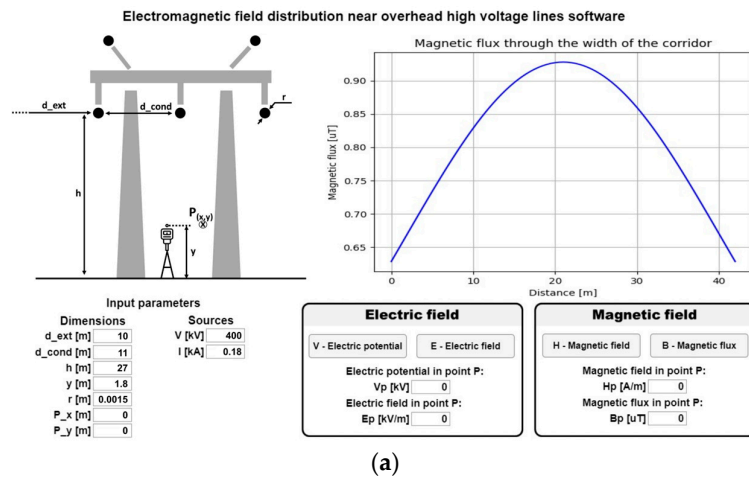


**Figure 14.** Cont.

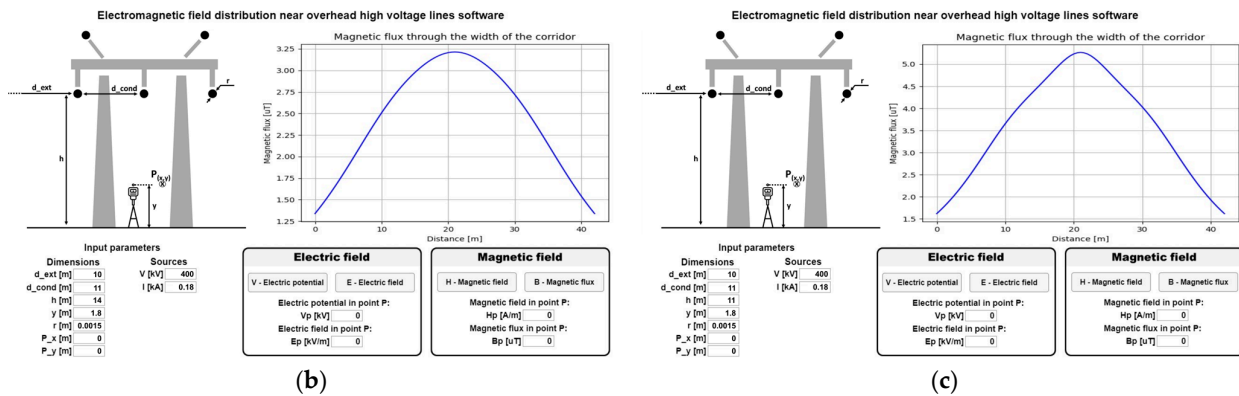


Figure 14. The magnetic induction distribution along the three paths, determined using the EMF program: (a) 1st path, h = 27 m; (b) 2nd path, h = 14 m; (c) 3rd path, h = 11 m, f = 50 Hz.

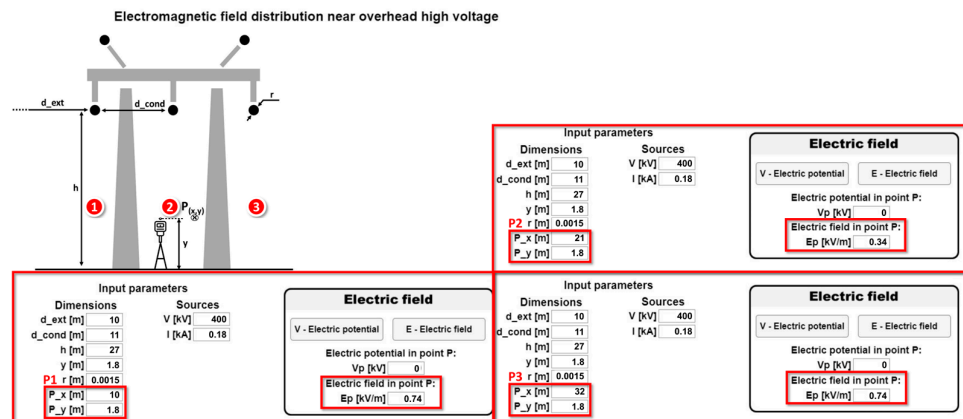


Figure 15. The electric field values in the three points of interest found using the EMF software program.

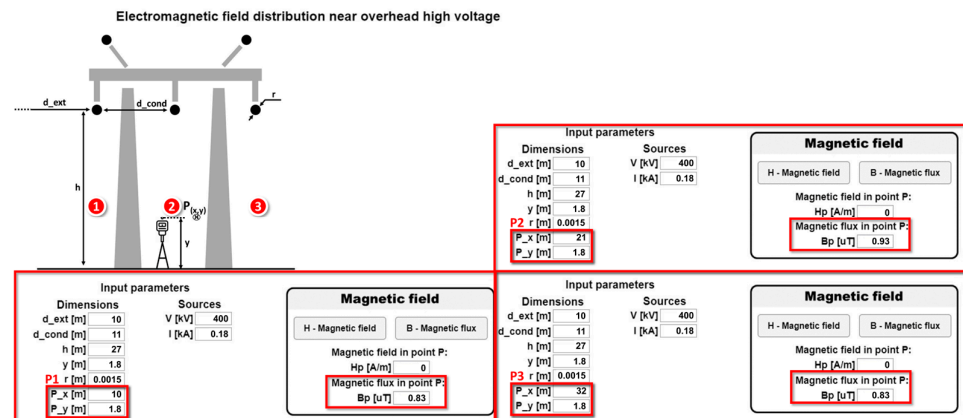
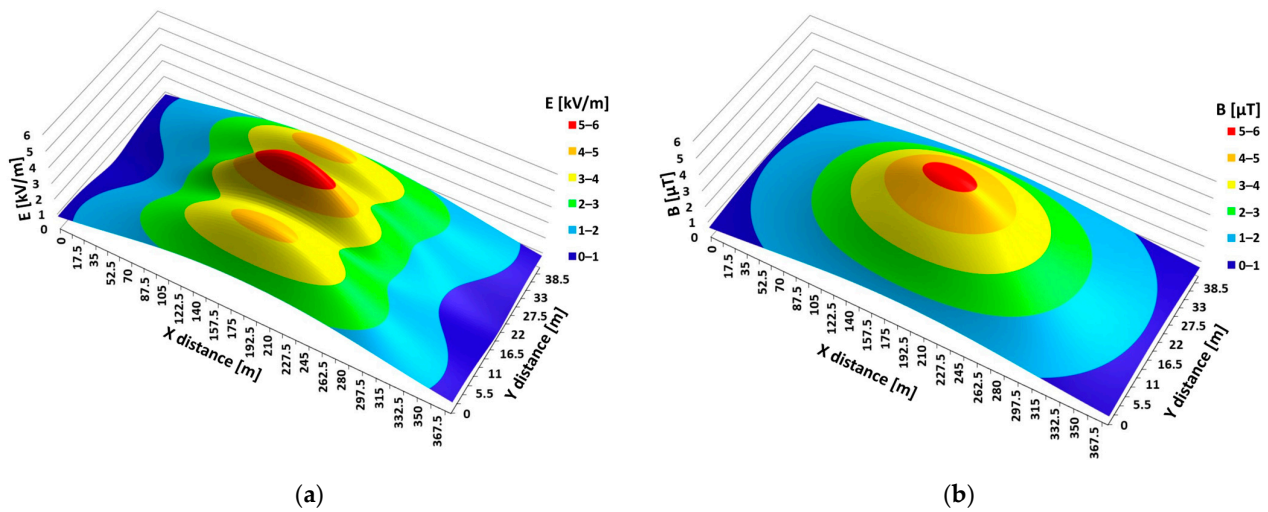


Figure 16. The magnetic field values in the three points of interest found using the EMF software program.

In the experimental EMC tests, when aiming to evaluate the exposure of humans to low-frequency electric and magnetic fields, the ability of the EMF program to determine the electric and magnetic field distributions on the area between two pillars (poles) is extremely useful, allowing us to predict the electric and magnetic field values before performing the experimental tests. In addition, because our program can be accessed on a mobile phone, such an evaluation of electric and magnetic fields can be started, with the distribution able to be determined on the ground immediately, as soon as the input data are identified (conductors' heights, distance between conductors, conductors' radii, electric voltage, current through the OHTL, etc.).



**Figure 17.** The field distribution in the area between two pillars (poles) of the 400 kV OHTL in Cluj-Napoca using the EMF program: (a) electric field; (b) magnetic field,  $f = 50$  Hz.

### 3.3. Determination of the Electric and Magnetic Fields Using ANSYS Maxwell 3D Software Program

To verify and validate the EMF software program developed by the authors, it was desirable to compare our software program results with the results obtained using a commercial software program dedicated to the numerical modelling of the electromagnetic field, namely ANSYS Maxwell 3D, version 2023. Therefore, to verify and validate the module dedicated to the electric field generated by the OHTL, determination was used for the AC Conduction module in which there were three projects implemented, one for each of the three paths of the 400 kV OHTL in Cluj-Napoca; these were analyzed both experimentally and using the EMF program. To exemplify this, the project corresponding to the 3rd path (area of maximum lines' sag) is presented in Figure 18; more precisely, this is the case in which it is considered that the three conductors are placed at a distance of 11 m from the ground.

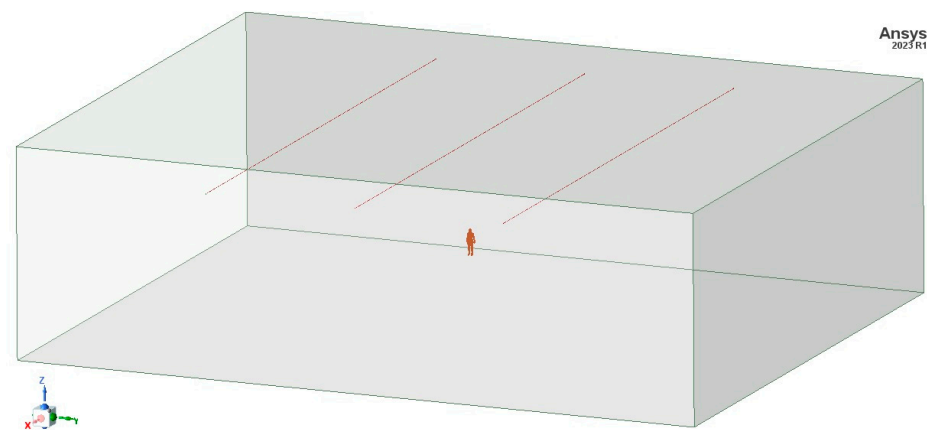


**Figure 18.** The model implemented in ANSYS.

In the image shown in Figure 18, it can be identified that the OHTL has three conductors in a horizontal configuration, placed with a distance of 11 m between them; the outline of a human body has a height of 1.8 m. In these projects, the region was not generated using the default function of the program, but was drawn so that the terminals of the three conductors attached to the region's faces were as presented in Figure 18, such that the program used to consider the OHTL conductors was infinitely long. For this, the boundary type was set to Even Symmetry on the two faces of the region that were attached to the

conductors. The three conductors were considered to have an ac voltage of 400 kV, and the base face of the region was set to 0 potential.

To analyze the electric field distribution along a path considered to be perpendicular on the three conductors, a line was drawn at 1.8 m from the ground, equal to the human body height, and then the distribution was performed on this line. In Figure 19, the electric field intensity distribution for the three paths of interest considered is presented.

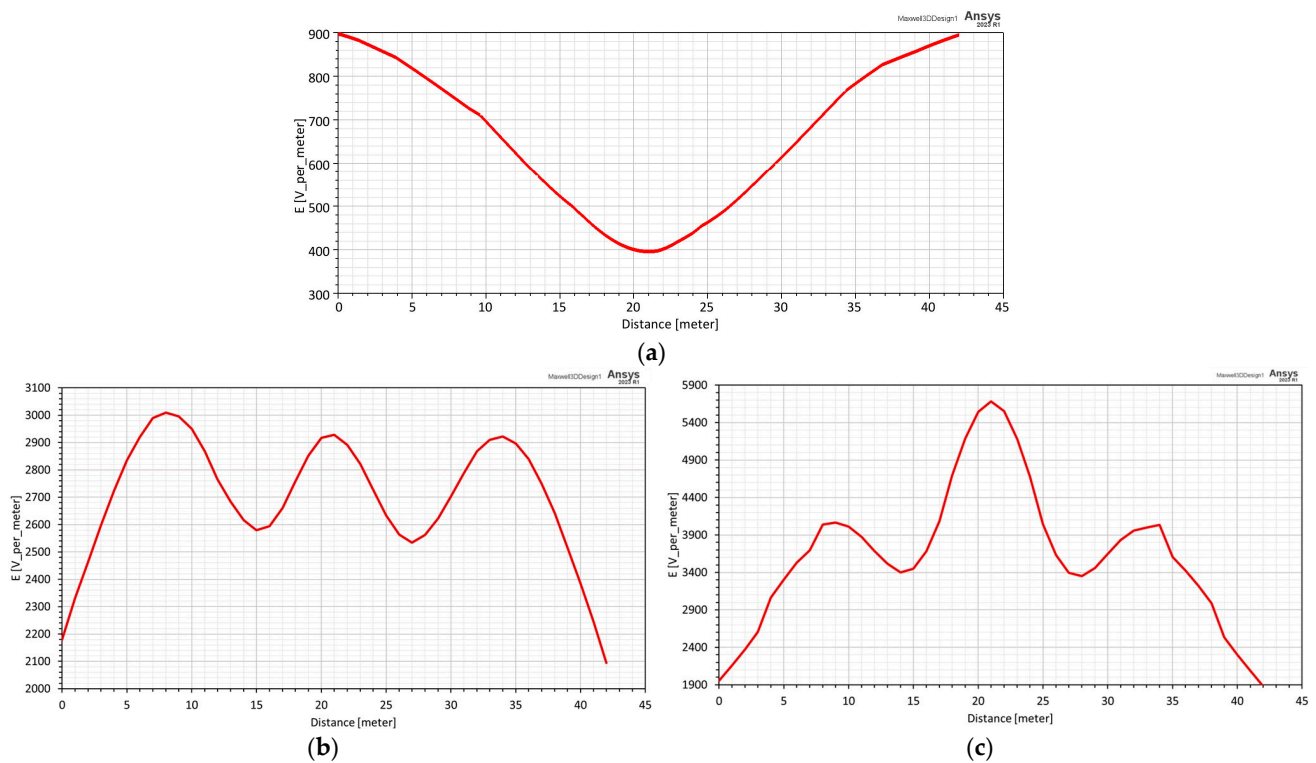


**Figure 19.** Electric field intensity distribution along the three paths found using the ANSYS Maxwell 3D software program: (a) 1st path,  $h = 27$  m; (b) 2nd path,  $h = 14$  m; (c) 3rd path,  $h = 11$  m,  $f = 50$  Hz.

In contrast to the ANSYS commercial software program, which can be used only on computers and involves the difficulty of drawing the 3D model, and difficult setups and analyses (complex models take a long time and need high computational resources), the EMF software program, designed and developed by the authors, has a very friendly interface, is more easily used, and it works also on mobile phones. Therefore, if we are in an HV station and in the process of evaluating the exposure of humans to electric and magnetic fields, and if, for example, at a measurement point, the values of the electric or magnetic field exceed the limits imposed by the standards in force [1,2], using the EMF software program, that value can be determined via analytical/numerical methods; in addition, whether this is the real field value or is an error of measurement or an error caused by other emissions sources, for example, other devices nearby in that area, can be verified.

Next, to also verify and validate the calculation algorithm for the magnetic field generated by the OHTL, using the EMF software program, three other projects were implemented; these corresponded to the three paths for calculation, in the ANSYS Maxwell 3D software program and in the Eddy Current module. The OHTL conductors were under a current of 180 A. The distributions of the magnetic induction along the paths are shown in Figure 20.

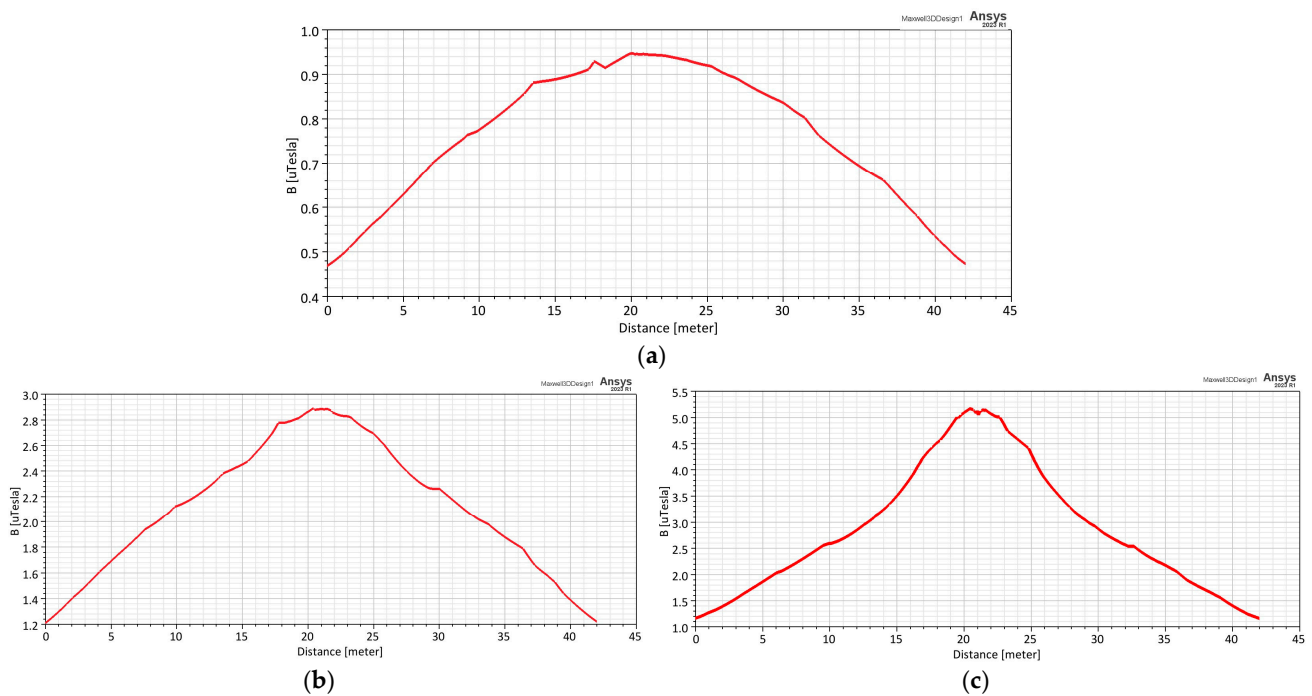


**Figure 20.** The magnetic induction distributions along the three paths found using the ANSYS Maxwell 3D software program: (a) 1st path,  $h = 27$  m; (b) 2nd,  $h = 14$  m; (c) 3rd path,  $h = 11$  m,  $f = 50$  Hz.

#### 4. Discussion

Further validations of the electric and magnetic fields computed with the EMF program developed by the authors and described in this article are required in order to assess the precision of the implemented mathematical model. Therefore, the accuracy of the EMF program results, e.g.,  $E$  and  $B$ , is assessed by comparing them with the experimental EMC tests measured on the 400 kV OHTL in Cluj-Napoca and the FEM results computed in the ANSYS Maxwell 3D commercial software program, respectively.

The results from the experimental measurements, EMF program, and Ansys are compared along the three measurement paths described in Section 3.1. The absolute relative error  $\varepsilon_r$  is chosen as the assessment metric, being computed between the (i) measurement and EMF program, and the (ii) Ansys results and EMF program, respectively, for all three paths.

First, the distribution of the electric field intensity is assessed. Comparisons along the 1st, 2nd, and 3rd measurement paths are shown in Figure 21a–c, respectively. It can be observed that the  $\varepsilon_r$  decreases with the OHTL height; thus, on the 3rd path, minimum  $\varepsilon_r$  values are obtained. The maximum  $\varepsilon_r$  is around 0.2 for both the measured and Ansys results. On the one hand, for the case of the measurements  $\varepsilon_r$ , important deviations can emerge due to physical influences (e.g., vegetation, terrain, OHTL steel structure). On the other hand, for the case of the Ansys  $\varepsilon_r$ , important deviations can emerge due to meshing and a domain region around the studied model.

Second, the distribution of the magnetic field intensity is assessed. Comparisons along the 1st, 2nd, and 3rd measurement paths are shown in Figure 22a–c, respectively.

It can be observed that the  $\varepsilon_r$  decreases with the OHTL height; thus, on the 3rd path, minimum  $\varepsilon_r$  values are obtained. In this case, the maximum  $\varepsilon_r$  is around 0.2 for both the measured and Ansys results, as in the previous case. The measurement  $\varepsilon_r$  values are smaller compared to the  $E$  measurement  $\varepsilon_r$ , with the maximum value being under 0.1 (10%).

Comparing the results obtained using the three methods, it can be observed that the experimental method, using the commercial software program ANSYS Maxwell 3D, and

using the EMF software program lead to similar results, which validates the software program developed and presented in this article by the authors.

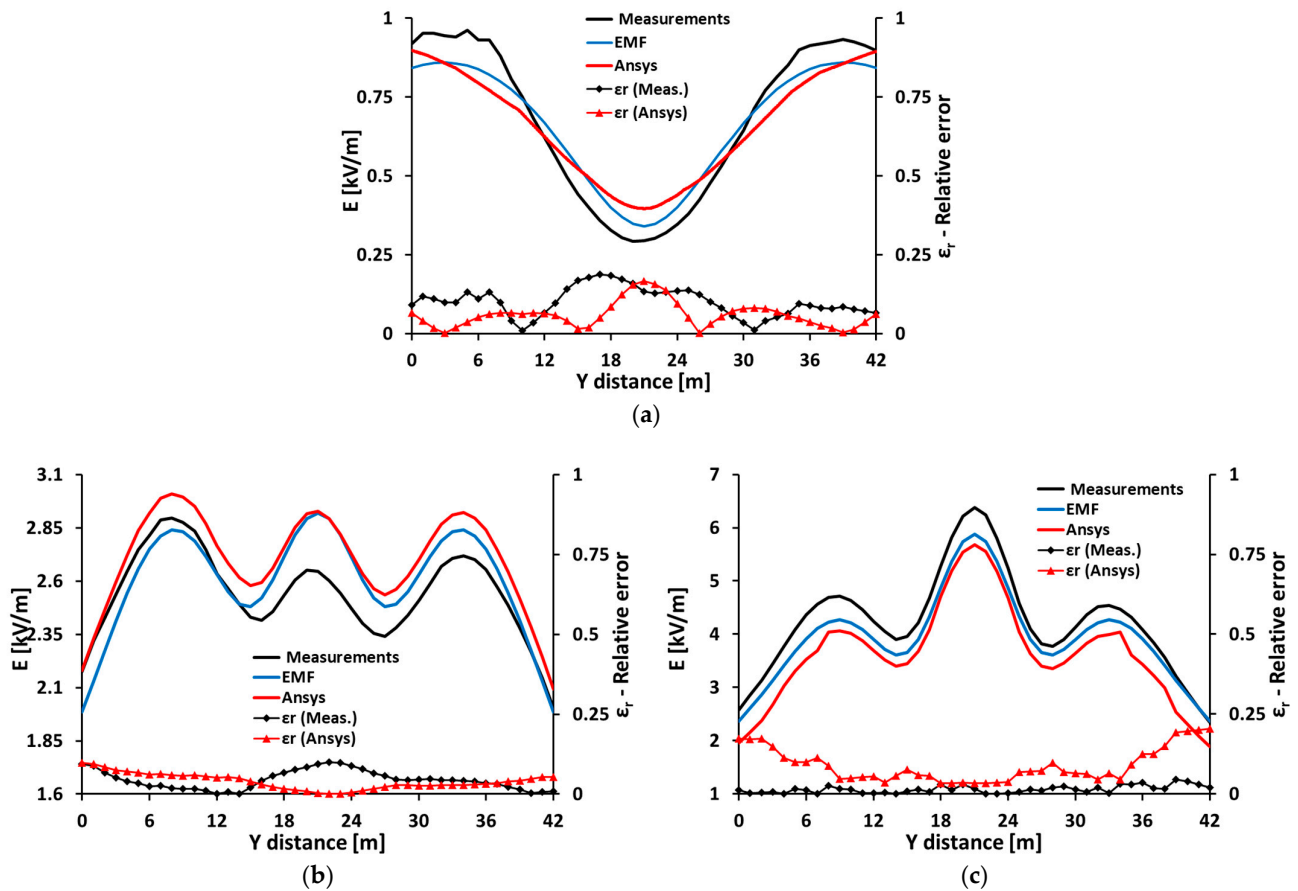


**Figure 21.** The electric field intensity distribution along the three paths was found experimentally, using the ANSYS Maxwell 3D program, and using the EMF program: (a) 1st path,  $h = 27$  m; (b) 2nd path,  $h = 14$  m; (c) 3rd path,  $h = 11$  m,  $f = 50$  Hz.

Analyzing the results obtained using the three different methods, we find that the values are in the limits imposed by the standards in force for professional exposure.

The major advantages of the EMF software program are that the results can be extracted with a high accuracy, the discretization is 0.1 to 0.1 m or smaller, and the user can impose the step for discretization; meanwhile, in general, in the process of EMC testing, measurements are performed from 3 to 3 m or in the best case, from 1 to 1 m.

Compared with other similar commercial software programs, our program is easier to use; takes less time to run; offers the possibility of post-processing the results in points, lines, surfaces, and 2D or 3D plots; has a very friendly interface; and can be used on smartphones. Also, the EMF software program allows users to determine the electric and magnetic field in an area between two OHTL poles, something that helps to previsualize the field distribution in a specific area before starting measurement testing. All these advantages make our EMF software program extremely useful in the process of evaluating the exposure of humans to the electric and magnetic fields emitted by OHTL conductors.

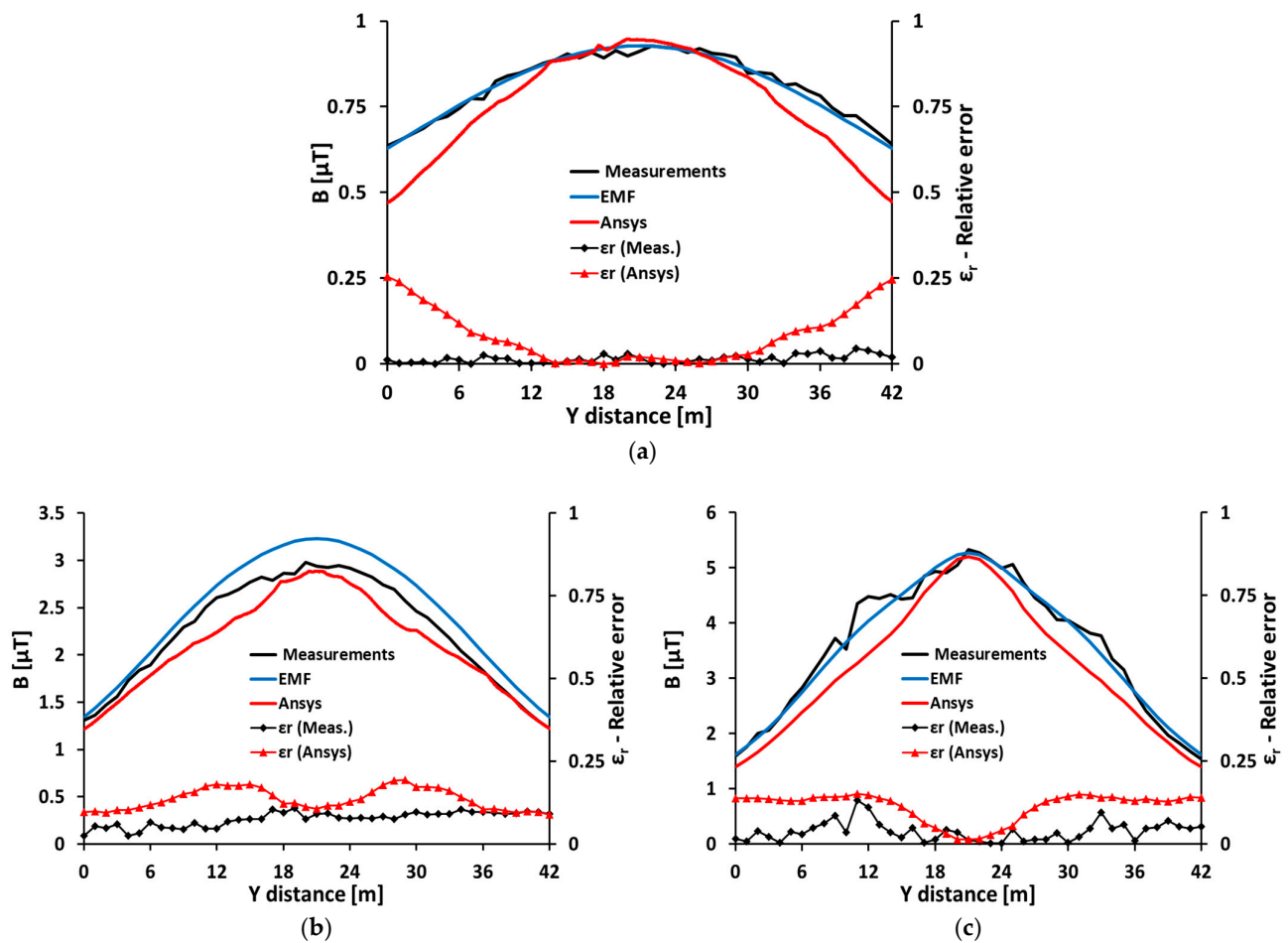


**Figure 22.** The magnetic field intensity distribution along the three paths found experimentally, using the ANSYS Maxwell 3D program, and using the EMF program: (a) 1st path,  $h = 27$  m; (b) 2nd path,  $h = 14$  m; (c) 3rd path,  $h = 11$  m,  $f = 50$  Hz.

## 5. Conclusions

This article proposes a software program dedicated to evaluating the exposure of humans to electric and magnetic fields, which is very useful in electromagnetic compatibility tests; this is because it allows the values of the electric and magnetic fields emitted by OHTLs to be quickly found and made available for use directly on smartphones. This means that the EMF software program can be used simultaneously with the experimental measurements directly at the place in which the measurements are made. The software program consists of two principal modules, one for the electric field and the other for the magnetic field, and each is based on a calculation algorithm. It is a very performant tool that can be useful in the process of EMC test digitalization.

The EMF software program was verified and validated by comparing the results with the experimental results and with those obtained using similar commercial programs. A 400 kV OHTL in Cluj-Napoca, Romania, was analyzed, and the results obtained using the EMF software program were compared with experimental tests and with those obtained using a commercial software program, ANSYS; this proved the precision and accuracy of our program. By comparing the results obtained from the three methods used for electric and magnetic field determination, the EMF software program accuracy can be observed, with the errors calculated being insignificant in most cases.

Using the EMF software program, we can determine electric and magnetic fields in a large number of points with a high accuracy, with less effort, and in a much shorter time than experimentally; thus, it is considered to be a welcome addition in the process of evaluating human exposure to electric and magnetic fields.

This EMF software program is part of a research program that aims to digitalize the process of evaluating human exposure to electric and magnetic fields.

**Author Contributions:** Conceptualization, A.G.; methodology, A.G.; software, A.G., A.B., C.M., C.P. and C.C.; validation, A.G., C.M. and V.T.; formal analysis, A.G., S.A. and M.G.; investigation, A.G., C.P., C.C. and M.G.; resources, A.G., S.A., A.B. and M.G.; data curation, A.G. and A.B.; writing—original draft preparation, A.G.; writing—review and editing, C.P. and C.C.; visualization, C.M. and V.T.; supervision, C.M. and V.T.; project administration, A.G.; funding acquisition, A.G. All authors have read and agreed to the published version of the manuscript.

**Funding:** This research was funded by the Academy of Romanian Scientists.

**Institutional Review Board Statement:** Not applicable.

**Informed Consent Statement:** Not applicable.

**Data Availability Statement:** Data are contained within the article.

**Acknowledgments:** This work was supported with a grant from the Academy of Romanian Scientists, project title: Digitalization of the Evaluation Process of Human Exposure to Electric and Magnetic Fields.

**Conflicts of Interest:** The authors declare no conflict of interest.

## References

1. Ordin nr. 1193 din 29 Septembrie 2006 Pentru Aprobarea Normelor Privind Limitarea Expunerii Populației Generale la Câmpuri Electromagnetice de la 0 Hz la 300 GHz. Available online: <https://legislatie.just.ro/Public/DetaliiDocumentAfis/76474> (accessed on 1 October 2023).
2. Hotărâre Nr. 520/2016 Din 20 Iulie 2016 Privind Cerințele Minime de Securitate și Sănătate Referitoare la Expunerea Lucrătorilor Lariscuri Generate de Câmpuri Electromagnetice. Available online: <https://adriaexpert.ro/hotararea-nr-520-2016-privind-cerintele-minime-de-securitate-si-sanatate-referitoare-la-expunerea-lucratorilor-la-riscuri-generate-de-campuri-electromagnetice> (accessed on 1 October 2023).
3. Gallego-Martínez, R.; Muñoz-Gutiérrez, F.J.; Rodríguez-Gómez, A. Trajectory Optimization for Exposure to Minimal Electromagnetic Pollution using Genetic Algorithms Approach: A Case Study. *Expert Syst. Appl.* **2022**, *207*, 118088. [[CrossRef](#)]
4. Bürgi, A.; Sagar, S.; Struchen, B.; Joss, S.; Rössli, M. Exposure Modelling of Extremely Low-Frequency Magnetic Fields from Overhead Power Lines and Its Validation by Measurements. *Int. J. Environ. Res. Public Health* **2017**, *14*, 949. [[CrossRef](#)] [[PubMed](#)]
5. Păcurar, C.; Țopa, V.; Giurgiuman, A.; Munteanu, C.; Constantinescu, C.; Gliga, M.; Andreica, S. The influence of the patch antennas emissions on the human head. In Proceedings of the IOP Conference Series: Materials Science and Engineering, ICEMS-BIOMED, Cluj-Napoca, Romania, 18–20 May 2022; pp. 1–14. [[CrossRef](#)]
6. Ghania, S.M.; Gharsallah, A. The potential effect of low-frequency EM fields on the human body. *J. Electr. Syst.* **2020**, *16*, 134–154.
7. Bonato, M.; Parazzini, M.; Chiaramello, E.; Fiocchi, S.; Le Brusquet, L.; Magne, I.; Souques, M.; Rössli, M.; Ravazzani, P. Characterization of Children’s Exposure to Extremely Low Frequency Magnetic Fields by Stochastic Modeling. *Int. J. Environ. Res. Public Health* **2018**, *15*, 1963. [[CrossRef](#)] [[PubMed](#)]
8. Fiocchi, S.; Liorni, I.; Parazzini, M.; Ravazzani, P. Assessment of Foetal Exposure to the Homogeneous Magnetic Field Harmonic Spectrum Generated by Electricity Transmission and Distribution Networks. *Int. J. Environ. Res. Public Health* **2015**, *12*, 3667–3690. [[CrossRef](#)] [[PubMed](#)]
9. Bottauscio, O.; Arduino, A.; Bavastro, D.; Capra, D.; Guarneri, A.; Parizia, A.; Zilberti, L. Exposure of Live-Line Workers to Magnetic Fields: A Dosimetric Analysis. *Int. J. Environ. Res. Public Health* **2020**, *17*, 2429. [[CrossRef](#)] [[PubMed](#)]
10. Gouda, O.E.; Amer, G.M.; Salem, W.A. Computational Aspects of Electromagnetic Fields near H.V. Transmission Lines. *Energy Power Eng.* **2009**, *1*, 65–71. [[CrossRef](#)]
11. Nedic, G.S.; Djuric, N.M.; Kljajic, D.R. The Comparison of EMF Monitoring Campaigns in Vicinity of Power Distribution Facilities. *ACES J.* **2022**, *37*, 129–139. [[CrossRef](#)]
12. Ali, E.; Memari, A.R. Effects of Magnetic Field of Power Lines and Household Appliances on Human and Animals and its Mitigation. In Proceedings of the Middle East Conference on Antennas and Propagation (MECAP), Cairo, Egypt, 20 October 2010.
13. Chervenkov, A. Modelling and Evaluation of Electromagnetic Field of urban High-voltage Power Line. In Proceedings of the International Conference on Energy Efficiency and Agricultural Engineering, Ruse, Bulgaria, 12–14 November 2020.
14. Ghania, S.M. Evaluation of Electromagnetic Fields Exposure during Live Line Working Conditions Inside High Voltage Substations. *Int. J. Eng. Sci. Technol.* **2013**, *3*.
15. Diamantis, A.; Kladas, A.G. Mixed Numerical Methodology for Evaluation of Low-Frequency Electric and Magnetic Fields Near Power Facilities. *IEEE Trans. Magn.* **2019**, *55*, 7000704. [[CrossRef](#)]
16. Mariscotti, A. Assessment of Human Exposure (Including Interference to Implantable Devices) to Low-Frequency Electromagnetic Field in Modern Microgrids, Power Systems and Electric Transports. *Energies* **2021**, *14*, 6789. [[CrossRef](#)]

17. Yamazaki, K. Assessment Methods for Electric and Magnetic Fields in Low and Intermediate Frequencies Related to Human Exposures and the Status of their Standardization. *Electron. Commun. Jpn.* **2020**, *103*, 10–18. [[CrossRef](#)]
18. Safigianni, A.S.; Tsompanidou, C.G. Electric- and Magnetic Field Measurements in an Outdoor Electric Power Substation. *IEEE Trans. Power Deliv.* **2009**, *24*, 38–42. [[CrossRef](#)]
19. Li, N.; Yang, X.; Peng, Z. Measurement of Electric Fields Around a 1000-kV UHV Substation. *IEEE Trans. Power Deliv.* **2013**, *28*, 2356–2362. [[CrossRef](#)]
20. Laakso, I.; Lehtinen, T. Modeling and Measurement of Exposure to Realistic Non-Uniform Electric Fields at 50 Hz. In Proceedings of the EMC Sapporo & APEMC 2019, Sapporo, Japan, 3–7 June 2009; pp. 334–337.
21. Munteanu, C.; Visan, G.; Pop, I.T.; Topa, V.; Merdan, E.; Racasan, A. Electric and Magnetic Field Distribution inside High and Very High Voltage Substations. In Proceedings of the 20th International Zurich Symposium on Electromagnetic Compatibility, Zurich, Switzerland, 27 February–3 March 2009; pp. 277–280.
22. Munteanu, C.; Visan, G.; Pop, I.T. Electric and Magnetic Field Distribution Inside High Voltage Power Substations. Numerical Modeling and Experimental Measurements. *IEEE Trans. Electr. Electron. Eng.* **2010**, *5*, 40–45. [[CrossRef](#)]
23. Virjoghe, E.O.; Bancuta, I.; Husu, A.G.; Cazacu, D.; Florescu, V. Measurement and Numerical Modelling of Electric Field in Open Type Air Substation. *J. Sci. Arts* **2019**, *46*, 249–259.
24. Fontgalland, G.; de Andrade, H.D.; de Figueiredo, A.L.; Queiroz, I.d.S., Jr.; De Oliveira, A.H.S.; Paiva, J.L.S.; Sousa, M.E.T. Estimation of electric and magnetic fields in a 230 kV electrical substation using spatial interpolation techniques. *IET Sci. Meas. Technol.* **2020**, *15*, 411–418. [[CrossRef](#)]
25. Daeri, A.; Hamoda, S. Effect of ELF Fields on Public Health Case Study (220 and 400 KV lines). In Proceedings of the International Maghreb Meeting of the Conference on Sciences and Techniques of Automatic Control and Computer Engineering MI-STA, Tripoli-Libya, Sabratah, Libya, 25–27 May 2021; pp. 623–626.
26. Mujezinović, A.; Čarsimamović, A.; Čarsimamović, S.; Muharemović, A.; Turković, I. Electric Field Calculation around of Overhead Transmission Lines in Bosnia and Herzegovina. In Proceedings of the 2014 International Symposium on Electromagnetic Compatibility, Gothenburg, Sweden, 1–4 September 2014.
27. Simion, E.; Maghiar, T. *Electrotehnica; Didactică și Pedagogică* Publisher: Bucharest, Romania, 1982.
28. Timotin, A.; Hortopan, V.; Ifrim, A.; Preda, M. *Lecții de Bazele Electrotehnicii; Didactică și Pedagogică* Publisher: Bucharest, Romania, 1970.
29. Pop, I.T.; Munteanu, C. *Analiza Distribuției de Camp Electric Si Magnetic in Statii Electrice de Inalta Tensiune*; Editura Politehnica: Timisoara, Romania, 2018.
30. Alihodzic, A.; Mujezinovic, A.; Turajlic, E.; Dedovic, M.M. Determination of Electric and Magnetic Field Calculation Uncertainty in the Vicinity of Overhead Transmission Lines. *J. Microw. Optoelectron. Electromagn. Appl.* **2022**, *21*, 392–413. [[CrossRef](#)]

**Disclaimer/Publisher’s Note:** The statements, opinions and data contained in all publications are solely those of the individual author(s) and contributor(s) and not of MDPI and/or the editor(s). MDPI and/or the editor(s) disclaim responsibility for any injury to people or property resulting from any ideas, methods, instructions or products referred to in the content.